The International Journal of Engineering and Science (IJES)
ISSN (e): 2319 – 1813 ISSN (p): 23-19 – 1805
|| Pages || PP 09-21 || 2020 ||

Melting Heat Transfer and Hall Currents on the Flow over an Exponentially Stretching Sheet with Thermal Radiation

Jagadeeshwar Pashikanti[1,*], Srinivasacharya Darbhashaynam[2]
[1] *Department of Mathematics, Indian Institute of Information Technology Tiruchirappalli, Tamil Nadu, India*
[2]*Department of Mathematics, National Institute of Technology Warangal, India*
[*]*Corresponding Author: jagadeeshwarp@iiitt.ac.in*

----------ABSTRACT----------
The present article analyses the significance of melting heat transfer in presence of Hall current on the laminar slip flow over an exponentially stretching surface in an electrically conducting incompressible viscous fluid. The numerical solutions to the governing equations are evaluated using a local similarity and non-similarity approach along with successive linearisation procedure and Chebyshev collocation method. The influence of pertinent parameters on the velocity, temperature, concentration, heat and mass transfer rates is analyzed. Tabular values for the skin-friction for the physical parameters are displayed. It is seen that increasing the value of melting parameter temperature and concentration reducing while, both the velocities increases. Moreover, a comparative analysis is conducted between the results obtained and known results in the literature for the specific values of the physical parameters, and are found to be in excellent agreement.
KEYWORDS: Heat and Mass transfer, Hall Current, Melting Condition.

I. INTRODUCTION

Owing to numerous applications in engineering and manufacturing process, the heat and mass transfer in the boundary layer flow of continuously stretching surfaces has attracted by many researchers. The cooling process of metallic sheets, crystal growth, the boundary layer along a liquid film condensation process, the aerodynamic extrusion of plastic sheets polymer and glass industries are some of applications of these flows.
The pioneering works of Sakiadis [1] motivated the several researchers to analyse the flow, heat and mass transfer characteristics of stretched flow problem via diverse physical conditions.

The Hall term representing the Hall current used to be overlooked as it has no outstanding result for small and average values of the applied magnetic field when applying the Ohm's law. The effects of Hall current are very predominant, when magnetic field of high strength is applied. The investigation of influence of Hall current theoretically on MHD flows has been given high priority as a result of its spreading applications in recent years such as in electric transformers, pumps and power generators, refrigeration coils, in flight MHD, Hall accelerators, cool combustors, electronic system cooling, thermal energy storage. Several researchers ([2 – 8] etc.) considered the flow problems with Hall Effect via various physical conditions and geometries.

Though there are some investigations on the heat and mass transfer along an exponentially stretching surface, the combined effects of Hall currents, melting condition and velocity slip have admitted no attention so far. Hence, in this article, we made an attempt to analyze these effects on the boundary layer flow, heat and mass transfer process over porous sheet stretching exponentially.

II. MATHEMATICAL FORMULATION

Consider a two dimensional laminar slip flow of electrically conducting viscous incompressible fluid with a temperature T_∞ and concentration C_∞ over an exponentially stretching permeable surface. The Cartesian framework is selected by taking positive $\tilde{x}-$axis along the sheet and $\tilde{y}-$axis orthogonal to the sheet as shown in the Fig. 1. The stretching velocity of the sheet is $U_*(\tilde{x}) = U_0\ e^{\tilde{x}/L}$., where U_0 is the reference velocity, $\tilde{x}$ is the distance from the slit and L is the reference length or scaling parameter. A magnetic field of strength $B(\tilde{x}) = B_0\ e^{\tilde{x}/2L}$, where B_0 is the constant magnetic field, is applied orthogonal to the sheet without neglecting the influence of Hall current. The assumption of small magnetic Reynolds number allows to neglect the induced magnetic field in contrast to applied magnetic field, due to which the flow becomes three dimensional. $(\tilde{u}_x, \tilde{u}_y, \tilde{u}_z)$ is the velocity vector, $\tilde{T}$ is the temperature and $\tilde{C}$ is the concentration. The suction/injection velocity of the fluid through the sheet is $V_0(\tilde{x}) = V_0\ e^{\tilde{x}/2L}$, where V_0 is the strength of suction/injection. Further, the slip velocity of the fluid is assumed as $N_*(\tilde{x}) = N_0\ e^{-\tilde{x}/2L}$, where N_0 is the

velocity slip factor. The fluid is considered to be a gray, absorbing/emitting radiation, but non-scattering medium. It is also assumed that the temperature of the melting surface is $T_m(\tilde{x})$ and concentration $C_m(\tilde{x})$. The Rosseland approximation [9] is used to describe the radiative heat flux in the energy equation.

Finally, we assume the fluid is isotropic, homogeneous, and has the scalar constant viscosity and electric conductivity. Hence, the above assumptions along with the Boussinesq and the boundary layer approximations, the present flow problem governed by the equations are given by

$$\frac{\partial \tilde{u}_x}{\partial \tilde{x}} + \frac{\partial \tilde{u}_y}{\partial \tilde{y}} = 0 \tag{1}$$

$$\tilde{u}_x \frac{\partial \tilde{u}_x}{\partial \tilde{x}} + \tilde{u}_y \frac{\partial \tilde{u}_x}{\partial \tilde{y}} = \nu \frac{\partial^2 \tilde{u}_x}{\partial \tilde{y}^2} + g\,\beta_T(\tilde{T} - T_m) + g\,\beta_C(\tilde{C} - C_m) - \frac{\sigma B^2}{\rho(1+\beta_h^2)}(\tilde{u}_x + \beta_h \tilde{u}_z) \tag{2}$$

$$\tilde{u}_x \frac{\partial \tilde{u}_z}{\partial \tilde{x}} + \tilde{u}_y \frac{\partial \tilde{u}_z}{\partial \tilde{y}} = \nu \frac{\partial^2 \tilde{u}_z}{\partial \tilde{y}^2} + \frac{\sigma B^2}{\rho(1+\beta_h^2)}(\beta_h \tilde{u}_x - \tilde{u}_z) \tag{3}$$

$$\tilde{u}_x \frac{\partial \tilde{T}}{\partial \tilde{x}} + \tilde{u}_y \frac{\partial \tilde{T}}{\partial \tilde{y}} = \alpha \frac{\partial^2 \tilde{T}}{\partial \tilde{y}^2} + \frac{16 T_\infty^3 \sigma^*}{3k^* \rho c_p} \frac{\partial^2 \tilde{T}}{\partial \tilde{y}^2} \tag{4}$$

$$\tilde{u}_x \frac{\partial \tilde{C}}{\partial \tilde{x}} + \tilde{u}_y \frac{\partial \tilde{C}}{\partial \tilde{y}} = D \frac{\partial^2 \tilde{C}}{\partial \tilde{y}^2} \tag{5}$$

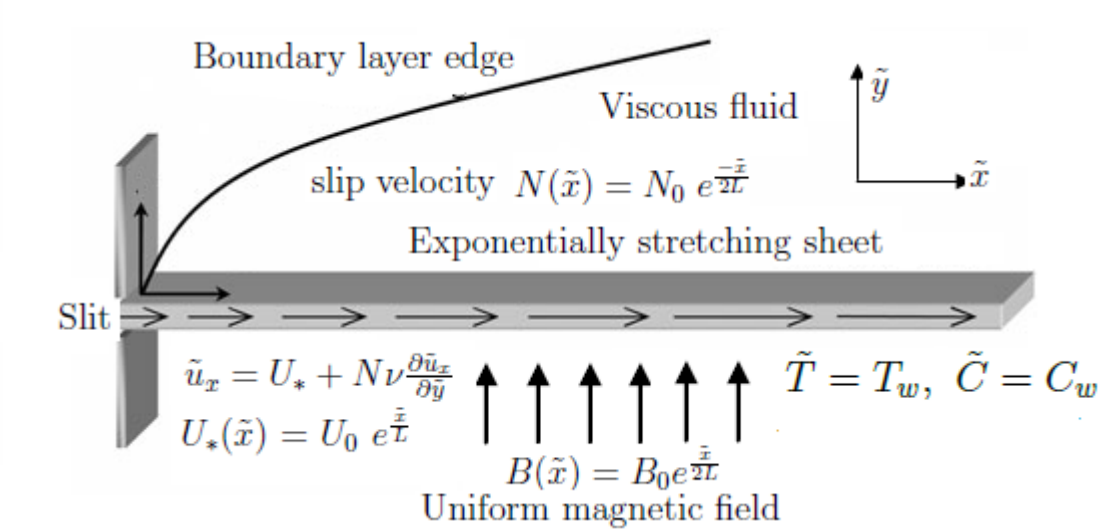

where β_h is Hall parameter, β_T is coefficient of thermal expansion, β_C is coefficient of solutal expansion, g is the acceleration due to gravity, σ is the electric conductivity, c_p is specific heat at the constant pressure, c_s is concentration susceptibility, ρ is density, ν is the kinematic viscosity of the fluid, D is the mass diffusivity and α is the thermal diffusivity.

The conditions on the surface of the sheet are

$$\left.\begin{aligned} &\tilde{u}_x = U_* + N_*\nu\frac{\partial \tilde{u}_x}{\partial \tilde{y}}, \tilde{u}_z = 0, \tilde{T} = T_m, \\ &\kappa\frac{\partial \tilde{T}}{\partial \tilde{y}} = \rho\left[\lambda_1 + c_s(T_m - T_0)\right](\tilde{u}_y + \beta(x,y)), \tilde{C} = C_m \quad \text{at} \quad \tilde{y} = 0 \\ &\tilde{u}_x \to 0, \tilde{u}_z \to 0, \tilde{T} \to T_\infty, \tilde{C} \to C_\infty \quad \text{as} \quad \tilde{y} \to \infty \end{aligned}\right\} \tag{6}$$

where $\beta(x,y) = V_0\, e^{-\tilde{x}/2L}$ and V_0 is a constant.

Introducing the following dimensionless variables

$$\left.\begin{aligned}
&\tilde{x} = xL, \tilde{y} = y\sqrt{\frac{2\nu L}{U_0}}e^{\frac{-\tilde{x}}{2L}}, \psi = \sqrt{2\nu L U_0}\,e^{\frac{\tilde{x}}{2L}}F(x,y),\\
&\tilde{u}_x = U_0 e^{\frac{\tilde{x}}{L}}F', \quad \tilde{u}_y = -\sqrt{\frac{\nu U_0}{2L}}\,e^{\frac{\tilde{x}}{2L}}(F + yF'), \quad \tilde{u}_z = U_0 e^{\frac{\tilde{x}}{L}}W(x,y)\\
&\tilde{T} = T_m + (T_\infty - T_m)T(x,y), \quad \tilde{C} = C_m + (C_\infty - C_m)C(x,y)
\end{aligned}\right\} \tag{7}$$

into Eqs. (1) – (5), we obtain

$$F''' + FF'' - 2F'^2 + 2Ri\,e^{-2x}(T + \mathrm{BC}) - \frac{H_a}{1+\beta_h^2}(F' + \beta_h W) + 2\left(F''\frac{\partial F}{\partial x} - F'\frac{\partial F'}{\partial x}\right) = 0 \tag{8}$$

$$W'' - 2F'W + FW' + \frac{H_a}{1+\beta_h^2}(\beta_h F' - W) + 2\left(W'\frac{\partial F}{\partial x} - F'\frac{\partial W}{\partial x}\right) = 0 \tag{9}$$

$$\frac{1}{Pr}\left(1 + \frac{4R}{3}\right)T'' + FT' + 2\left(T'\frac{\partial F}{\partial x} - F'\frac{\partial T}{\partial x}\right) = 0 \tag{10}$$

$$\frac{1}{Sc}C'' + FC' + 2\left(C'\frac{\partial F}{\partial x} - F'\frac{\partial C}{\partial x}\right) = 0 \tag{11}$$

The corresponding boundary conditions reduce to

$$\left.\begin{aligned}
&F'(x,0) = 1 + \lambda F''(x,0), W(x,0) = 0, \quad T(x,0) = 0,\\
&M_w T'(x,0) + PrF(x,0) + 2Pr\frac{\partial F}{\partial x}(x,0) = Pr\,S, C(x,0) = 0,\\
&F'(x,y) \to 0, W(x,y) \to 0, T(x,y) \to 1, C(x,y) \to 1 \text{ as } \quad y \to \infty
\end{aligned}\right\} \tag{12}$$

where S = $V_0\sqrt{2L/\nu U_0}$ is the suction or injection parameter according as S > 0 or S < 0 respectively, *Sc = ν/D* is the Schmidt number, λ = $N_0\sqrt{\nu U_0/2L}$ is the velocity slip parameter, Pr = ν/α is the Prandtl number, Re = U_0 L/ν, Gr = g β_T T_0 L^3/ ν^2 and Ri = Gr/Re^2 are the Reynold's, Grashof number and Richardson numbers, respectively, R = $4\sigma^* T_\infty^3$ /k k* is the radiation parameter, $B = \beta_C (C_\infty - C_m)/\beta_T (T_\infty - T_m)$ is the buoyancy ratio and the prime denotes derivative with respect to *y*.

The non-dimensional skin friction in $\tilde{x}$-direction $C_{F\tilde{x}} = 2\tau_{\omega\tilde{x}}/\rho U_*^2$, local skin-friction in $\tilde{z}-$direction $C_{F\tilde{z}} = 2\tau_{\omega\tilde{z}}/\rho U_*^2$, the local Nusselt number $Nu_{\tilde{x}} = \tilde{x}q_w/\kappa(T_\infty - T_m)$ and local Sherwood number $Sh_{\tilde{x}} = \tilde{x}q_m\kappa(C_\infty - C_m)$, are given by

$$\left.\begin{aligned}
&\frac{\sqrt{Re_x}}{\sqrt{2x/L}}C_{F\tilde{x}x} = F''(x,0), \quad \frac{\sqrt{Re_x}}{\sqrt{2x/L}}C_{F\tilde{z}x} = W'(x,0),\\
&\frac{Nu_x}{\sqrt{Lx/2}\sqrt{Re_x}} = -\left(1 + \frac{4R}{3}\right)T'(x,0) \text{ and } \frac{Sh_x}{\sqrt{Lx/2}\sqrt{Re_x}} = -C'(x,0)
\end{aligned}\right\} \tag{13}$$

where Re_x = x $U_*(x)$ / ν is the local Reynolds number.

III. NUMERICAL SOLUTION

The numerical solutions to Eqs. (8) to (11) together with Eq. (12) are evaluated using a local similarity and non-similarity method [10], successive linearisation and then pseudo spectral method ([11], [12]).

III(i). LOCAL NON-SIMILARITY METHOD

The initial approximate solution can be obtained from the local similarity equations for a particular case x<<1 by suppressing the terms $x(\partial/\partial x)$. As there are no terms accompanied with $x(\partial/\partial x)$ in (8) – (11), there is no change in the governing equations and boundary conditions.

In the second step, introduce $G=\partial F/\partial x$, $H=\partial W/\partial x$, $J=\partial T/\partial x$ and $K=\partial C/\partial x$ to get back the suppressed terms in the first step. Thus the second level truncation is

$$F'''+FF''-2F'^2+2Ri\,e^{-2x}(T+\mathrm{BC})-\frac{H_a}{1+\beta_h^2}(F'+\beta_h W)+2\left(F''G-F'G'\right)=0 \tag{14}$$

$$W''-2F'W+FW'+\frac{H_a}{1+\beta_h^2}(\beta_h F'-W)+2\left(W'G-F'H\right) \tag{15}$$

$$\frac{1}{Pr}\left(1+\frac{4R}{3}\right)T''+FT'+2\left(T'G-F'J\right)=0 \tag{16}$$

$$\frac{1}{Sc}C''+FC'+2\left(C'G-F'K\right)=0 \tag{17}$$

The associated boundary conditions are

$$\left.\begin{aligned}&F'(x,0)=1+\lambda F''(x,0),\quad W(x,0)=0,\quad T(x,0)=0,\\&M_w T'(x,0)+PrF(x,0)+2PrG(x,0)=PrS,,\quad C(x,0)=0,\\&F'(x,y)\to 0,W(x,y)\to 0,T(x,y)\to 1,C(x,y)\to 1\ \text{ as }\ y\to\infty\end{aligned}\right\} \tag{18}$$

In the third step, differentiate Eqs. (14) – (17) with respect to *x* and neglect terms accompanied with $\partial G/\partial x$, $\partial H/\partial x$, $\partial J/\partial x$ and $\partial K/\partial x$, then we get

$$\left.\begin{aligned}&G'''+FG''+GF''-4F'G'+2Ri\,e^{-2x}\left(J+\mathrm{B}K-2T-2\mathrm{BC}\right)\\&-\frac{H_a}{1+\beta_h^2}\left(G'+\beta_h H\right)+2\left(G''G-G'^2\right)=0\end{aligned}\right\} \tag{19}$$

$$H''-2\left(G'W+F'H\right)+GW'+FH'+\frac{H_a}{1+\beta_h^2}\left(\beta_h G'-H\right)+2\left(H'G-G'H\right)=0 \tag{20}$$

$$\frac{1}{Pr}\left(1+\frac{4R}{3}\right)J''+GT'+FJ'+2\left(J'G-G'J\right)=0 \tag{21}$$

$$\frac{1}{Sc}K''+FK'+GC'+2\left(K'G-G'K\right)=0 \tag{22}$$

The associated boundary conditions are

$$\left.\begin{aligned}&G'(x,0)=\lambda\,G''(x,0),H(x,0)=0,J(x,0)=0,\\&M_w J'(x,0)+PrG(x,0)=0,K(x,0)=0\\&G'(x,\infty)\to 0,H(x,\infty)\to 0,J(x,\infty)\to 0,K(x,\infty)\to 0\end{aligned}\right\} \tag{23}$$

III(ii). LOCAL NON-SIMILARITY METHOD

Let $\Gamma(y)=[F,W,T,C,G,H,J,K]$ and assume that

$$\Gamma(y)=\Gamma_i(y)+\sum_{r=0}^{i-1}\Gamma_r(y) \tag{24}$$

where $\Gamma_i(y)$ (i=1,2,3,...) are unknown functions that are determined by recursively evaluating the linearised version of the (14) to (23) after introducing Eq. (24) into them and $\Gamma_r(y)$ $(r\geq 1)$ are known functions determined from previous iterations.

$$\left.\begin{aligned}&F_i'''+\chi_{11,i-1}F_i''+\chi_{12,i-1}F_i'+\chi_{13,i-1}F_i-\frac{H_a\,\beta_h}{1+\beta_h^2}W_i+2Ri\,e^{-2x}(T_i+\mathrm{BC}_i)\\&+\chi_{14,i-1}G_i'+\chi_{15,i-1}G_i=\zeta_{1,i-1}\end{aligned}\right\} \tag{25}$$

$$\chi_{21,i-1}F_i'+\chi_{22,i-1}F_i+W_i''+\chi_{23,i-1}W_i'+\chi_{24,i-1}W_i+\chi_{25,i-1}G_i+\chi_{26,i-1}H_i=\zeta_{2,i-1} \tag{26}$$

$$\chi_{31,i-1}F_i' + \chi_{32,i-1}F_i + \frac{1}{Pr}\left(1+\frac{4R}{3}\right)T_i'' + \chi_{33,i-1}T_i' + \chi_{34,i-1}G_i + \chi_{35,i-1}J_i = \zeta_{3,i-1} \tag{27}$$

$$\chi_{41,i-1}F_i' + \chi_{42,i-1}F_i + \frac{1}{Sc}C_i'' + \chi_{43,i-1}C_i' + \chi_{44,i-1}G_i + \chi_{45,i-1}K_i = \zeta_{4,i-1} \tag{28}$$

$$\left.\begin{aligned} &\chi_{51,i-1}F_i'' + \chi_{52,i-1}F_i' + \chi_{53,i-1}F_i + (-4Ri\, e^{-2x})(T_i + \mathrm{B}C_i) + G_i''' + \chi_{54,i-1}G_i'' \\ &+\chi_{55,i-1}G_i' + \chi_{56,i-1}G_i - \frac{H_a\,\beta_h}{1+\beta_h^2}H_i + (2Ri\, e^{-2x})J_i + (2\mathrm{B}Ri\, e^{-2x})K_i = \zeta_{5,i-1} \end{aligned}\right\} \tag{29}$$

$$\left.\begin{aligned} &\chi_{61,i-1}F_i' + \chi_{62,i-1}F_i + \chi_{63,i-1}W_i' + \chi_{64,i-1}W_i + \chi_{65,i-1}G_i' + \chi_{66,i-1}G_i + H_i'' \\ &+\chi_{67,i-1}H_i' + \chi_{68,i-1}H_i = \zeta_{6,i-1} \end{aligned}\right\} \tag{30}$$

$$\left.\begin{aligned} &\chi_{71,i-1}F_i + \chi_{72,i-1}T_i' + \chi_{73,i-1}G_i' + \chi_{74,i-1}G_i + \frac{1}{Pr}\left(1+\frac{4R}{3}\right)J_i'' + \chi_{75,i-1}J_i' \\ &+\chi_{76,i-1}J_i = \zeta_{7,i-1} \end{aligned}\right\} \tag{31}$$

$$\chi_{81,i-1}F_i + \chi_{82,i-1}C_i' + \chi_{83,i-1}G_i' + \chi_{84,i-1}G_i + \frac{1}{Sc}K_i'' + \chi_{85,i-1}K_i' + \chi_{86,i-1}K_i = \zeta_{8,i-1} \tag{32}$$

where the coefficients $\chi_{lk,n-1}$ and $\zeta_{k,i-1}$, (l, k = 1, 2, 3,..., 8) are in terms of the approximations F_i, W_i, T_i and C_i, (i = 1,2,3,..., $\overline{n-1}$) and their derivatives.

III(iii). CHEBYSHEV COLLOCATION METHOD

The linearized equations obtained in section III(ii) are solved using the Chebyshev collocation procedure [12]. In view of numerical computations, the region [0, ∞) is truncated to [0, L] for large *L*, where *L* is the scaling parameter. In order to apply Chebyshev collocation procedure, the interval [0, L] is converted to [-1, 1] by the mapping

$$\tilde{\tau} = \frac{2y}{L} - 1, \quad -1 \le \tilde{\tau} \le 1 \tag{33}$$

The unknown functions $\Gamma_i(y)$ (i=1,2,3,...) and their derivatives expressed in terms of Chebyshev polynomials $\mathrm{Y}_k(\tilde{\tau}) = \cos(k\cos^{-1}(\tilde{\tau}))$ at Gauss-Lobatto collocation points $\tilde{\tau}_m = \cos(\pi m / N)$, m = 0,1,2,. . .,N as

$$\Gamma_i(\tilde{\tau}) = \sum_{k=0}^{N}\Gamma_i(\tilde{\tau}_k)\mathrm{Y}_k(\tilde{\tau}_m), \quad \text{and} \quad \frac{d^{\mathbf{a}}\Gamma_r}{dy^{\mathbf{a}}} = \sum_{k=0}^{N}\mathbf{D}_{\mathbf{km}}^{\mathbf{a}}\Gamma_i(\tilde{\tau}_k) \tag{34}$$

where $\mathbf{D} = 2\mathrm{D}/L$ with D is the Chebyshev derivative matrix and **a** is the order of the derivative. Substitution of Eq. (34) in Eqs. (25) to (32) gives

$$\mathrm{A}_{i-1}\mathrm{X}_i = \square_{i-1}, \tag{35}$$

where A_{i-1} is a 8th order square matrix with elements as (N + 1)th order square matrices in terms of the coefficients χ_{ij}'s. X_i and $\square_{i-1}$ are 8th order column vectors with $(N+1)\times 1$ column vectors as elements in terms of $\Gamma_i(\tilde{\tau}_k)$ and $\chi_{s,i-1}$. Hence, the solution can be obtained by solving the matrix system (35), after implementing the boundary conditions.

IV. RESULTS AND DISCUSSION

To elucidate the significance of relevant parameters, the numerical calculations are carried out by taking Sc = 0.22, Pr = 1.0, B = 0.5, S = 0.5, Ri = 0.1, β_h = 0.5$, $\mathrm{H_a}$ = 0.5, $\mathrm{M_w}$ = 0.5, λ = 1.00, R = 0.5, x = 0.2, N = 100 and L = 20 unless otherwise mentioned.

The variation of tangential velocity with the influence of β_h, $\mathrm{M_w}$, R, λ and S is shown in the Figs. 2(a) – 2(e). Increase in the value of Hall and melting parameters enhances the velocity of the fluid as shown in the Fig. 2(a) and 2(b). It is noticed in the Figs. 2(c) and 2(d) that the fluid velocity diminishes with increase in the value of thermal radiation and velocity slip parameters. Figure 2(e) narrates that the fluid velocity in the boundary layer reduces with wall fluid suction. This is due to the fact that the wall suction has the tendency to reduce the momentum boundary.

Figures 3(a) – 3(e) represents the variations of the transverse velocity for distinct values of β_h, M_w, R, λ and S, respectively. It is noticed from the Fig. 3(a), that there is no secondary flow velocity in the absence of Hall parameter. As the values of β_h increase, the cross flow is generated and reaches to a maximum for every profile and then falls to zero. It is noticed form the Figs. 3(b) and that the transverse velocity increases with increase in the value of melting parameter. While, an opposite trend is noticed with increase in the thermal radiation as shown in the Fig. 3(c). Figures 3(d) and 3(e) exhibits that the transverse velocity decreases with the increase in slipperiness and wall fluid suction.

Figures 4(a) – 4(e) are due to the variation of temperature profile for distinct values of β_h, M_w, R, λ and S. An enhancement in the value of β_h, the effective thermal conductivity of the fluid escalates and hence temperature enhances as shown in the Fig. 4(a). It is observed from Fig. 4(b) that the temperature decreases with enhance in the value of M_w. The effective convective potential flow between the melting surface and ambient fluid in the medium reduces with increase in the thermal radiation parameter. Therefore, temperature of the fluid reduces in the boundary layer as portrayed in the Fig. 4(c). Figures 4(d) and 4(e) shows that the fluid temperature decreases with velocity slip and enhances with fluid suction.

The variation of concentration profile for distinct values of β_h, M_w, R, λ and S is portrayed in the Figs. 5(a) – 5(e). From Figs. 5(a) and 5(b), it is seen that the concentration increases as strengthening the Hall parameter and reduces by strengthening the melting parameter. As the values of radiation parameter escalates, concentration boundary layer enhances and hence, concentration rises as shown in the Fig. 5(c). It is observed that the concentration reduces with velocity slip at the boundary and increases with fluid suction as shown in the Figs. 5(d) and 5(e), respectively.

The influence of β_h, M_w, R, λ and S on the rate of heat absorption against non-similar variable x is explored in the Figures 6(a) – 6(e). It is observed from the Fig. 6(a) that the rate of heat absorption enhances with an increase in the value of Hall parameter. As expected, enhancing the value of melting parameter M_w, the rate of heat absorption decreases as portrayed in the Fig. 6(b). The rate of heat absorption increases with an increase in the value of thermal radiation parameter R as depicted in the Fig. 6(c). Further, in the absence of thermal radiation, minimum rate of heat absorption occurred and as strengthening the radiation, the rate of heat absorption increased as shown in the Fig. 6(c). The effect of λ on the rate of heat absorption is presented in the Fig. 6(d). It is evident from the figure that the rate of heat absorption reduces with an increase in velocity slip parameter λ. Figure 6(e) shows that the rate of heat absorption increases with an increase in the fluid suction at the boundary of the stretching surface.

The influence of β_h, M_w, R, λ and S on the rate of mass absorption against non-similar variable x is explored in the Figures 7(a) – 7(e). It is observed from the Fig. 7(a) that the rate of mass absorption increases with an increase in the value of β_h. As expected, enhancing the value of M_w, the rate of mass absorption decreases as portrayed in the Fig. 7(b). The rate of mass absorption increases with an increase in the value of thermal radiation parameter R as depicted in the Fig. 7(c). Further, in the absence of thermal radiation, minimum rate of mass absorption occurred and as strengthening the thermal radiation, the rate of mass absorption increased as shown in the Fig. 7(c). The effect of λ on the rate of mass absorption is presented in the Fig. 7(d). It is evident from the figure that the rate of mass absorption decreases with a raise in λ. Figure 7(e) shows that the rate of mass absorption enhances with a raise in the fluid suction.

The variations of F"(x,0) and W'(x,0) for diverse values of pertinent parameters are tabulated in Table (1). It is displayed in the table that, both the skin-friction F"(x,0) and W'(x,0) reduces with fluid suction. Table (1) shows that, the skin-friction in both directions are increasing in presence of Hall and melting parameter, which results in reducing the boundary layer and therefore, higher velocity gradient at the surface. On the other hand, both the skin-friction reduces with increase in thermal radiation parameter. Increase in the velocity slip, skin-friction in $\tilde{x}$-direction increases and decreases in $\tilde{z}$-direction. While, an opposite trend is observed in presence of magnetic parameter H_a.

V. CONCLUSIONS

This article addresses the effect of radiative melting heat transfer on the laminar slip flow due to incompressible viscous fluid on a porous stretching sheet in presence of Hall effect. A local similarity and non-similarity method along with successive linearization together with Chebyshev spectral collocation method is used to find the solution of the governing equations. The main conclusions of the present study are as follows.

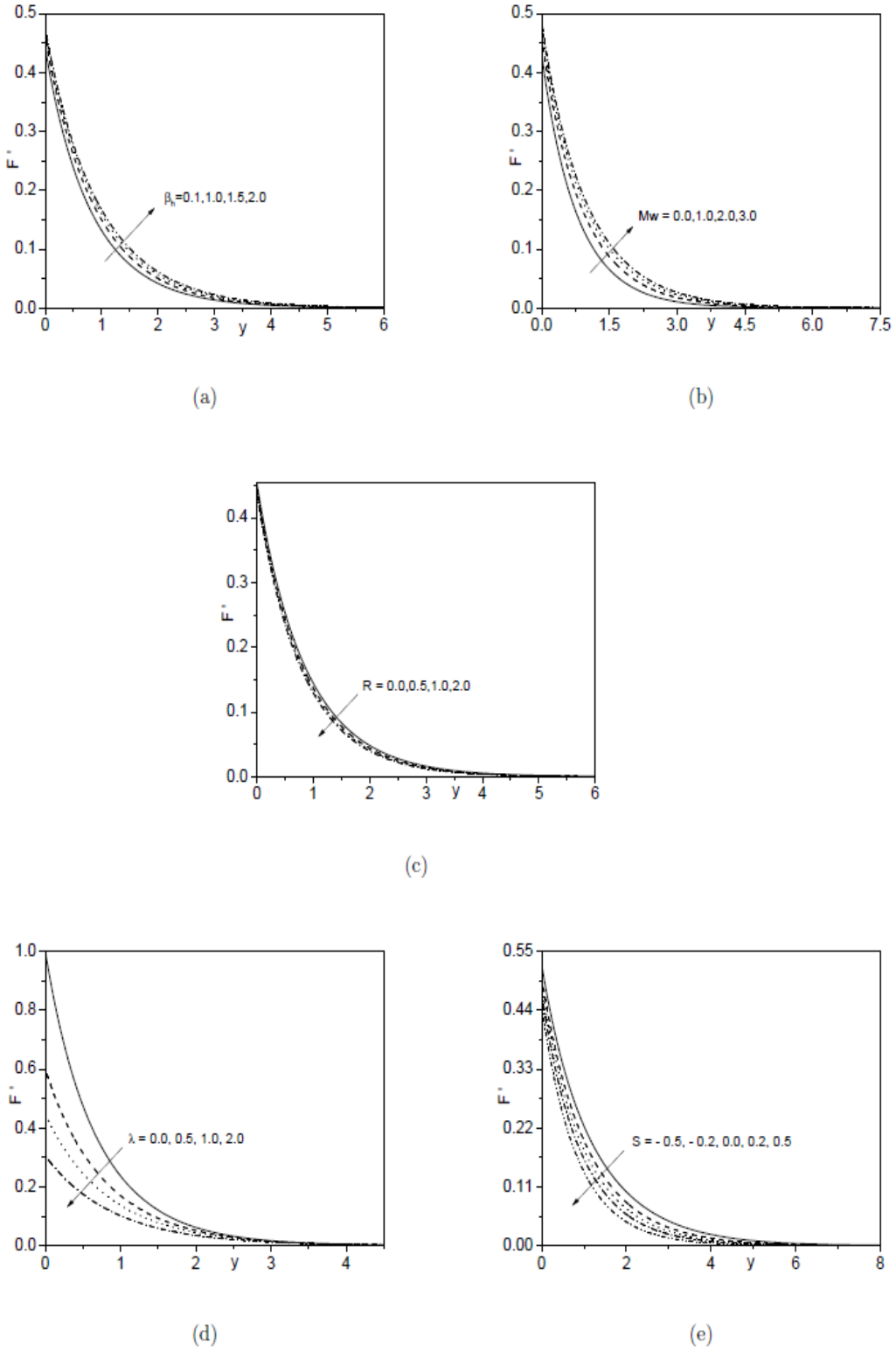

(a) (b)

(c)

(d) (e)

Figure 2: Influence of (a) β_h (b) Mw, (c) R, (d) λ and (e) S on F'.

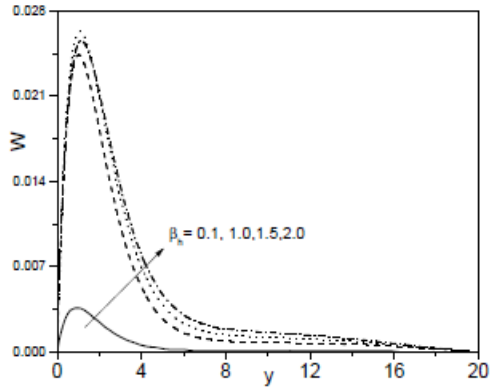

(a)

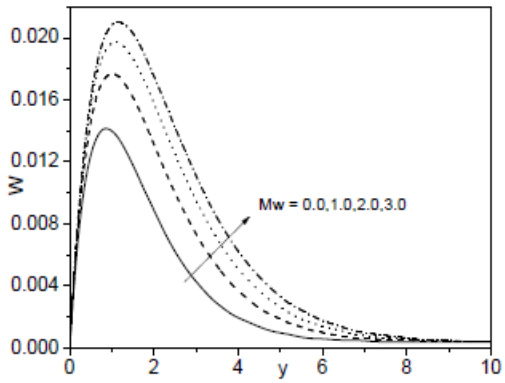

(b)

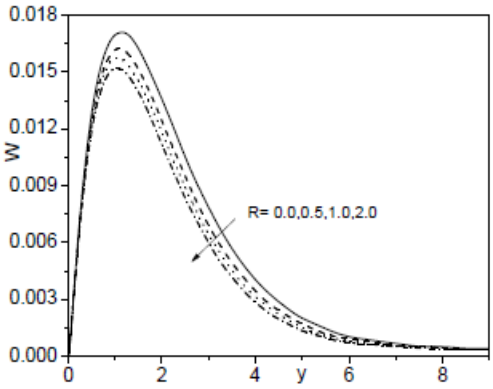

(c)

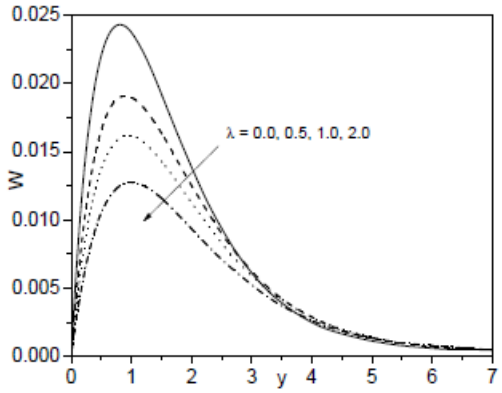

(d)

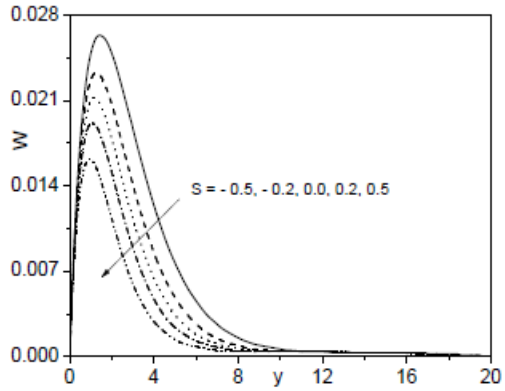

(e)

Figure 3: Influence of (a) β_h (b) Mw, (c) R, (d) λ and (e) S on W.

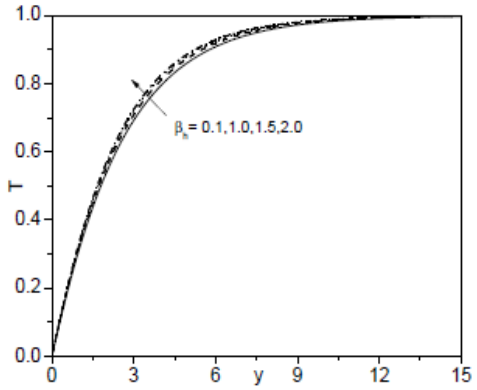

(a)

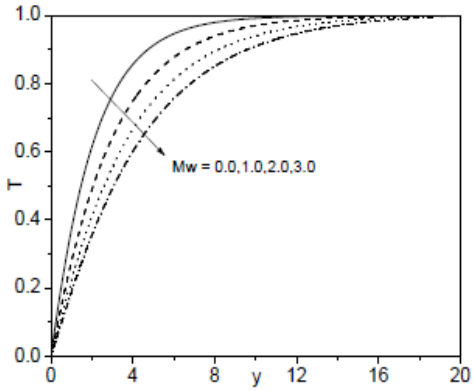

(b)

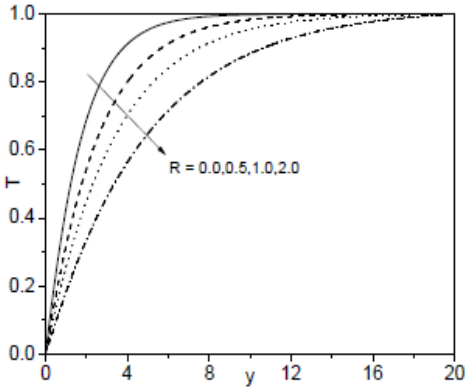

(c)

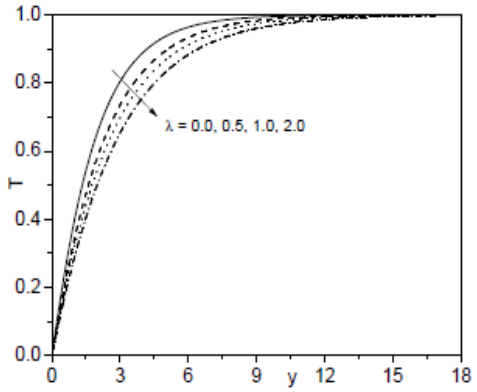

(d)

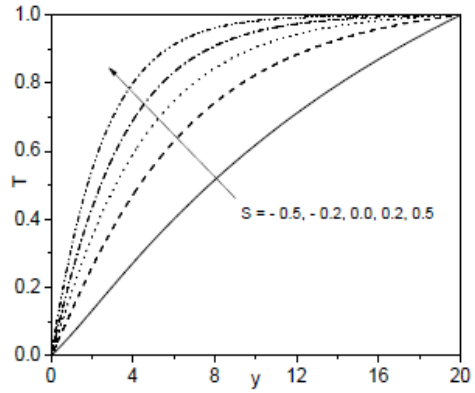

(e)

Figure 4: Influence of (a) β_h (b) Mw, (c) R, (d) λ and (e) S on T.

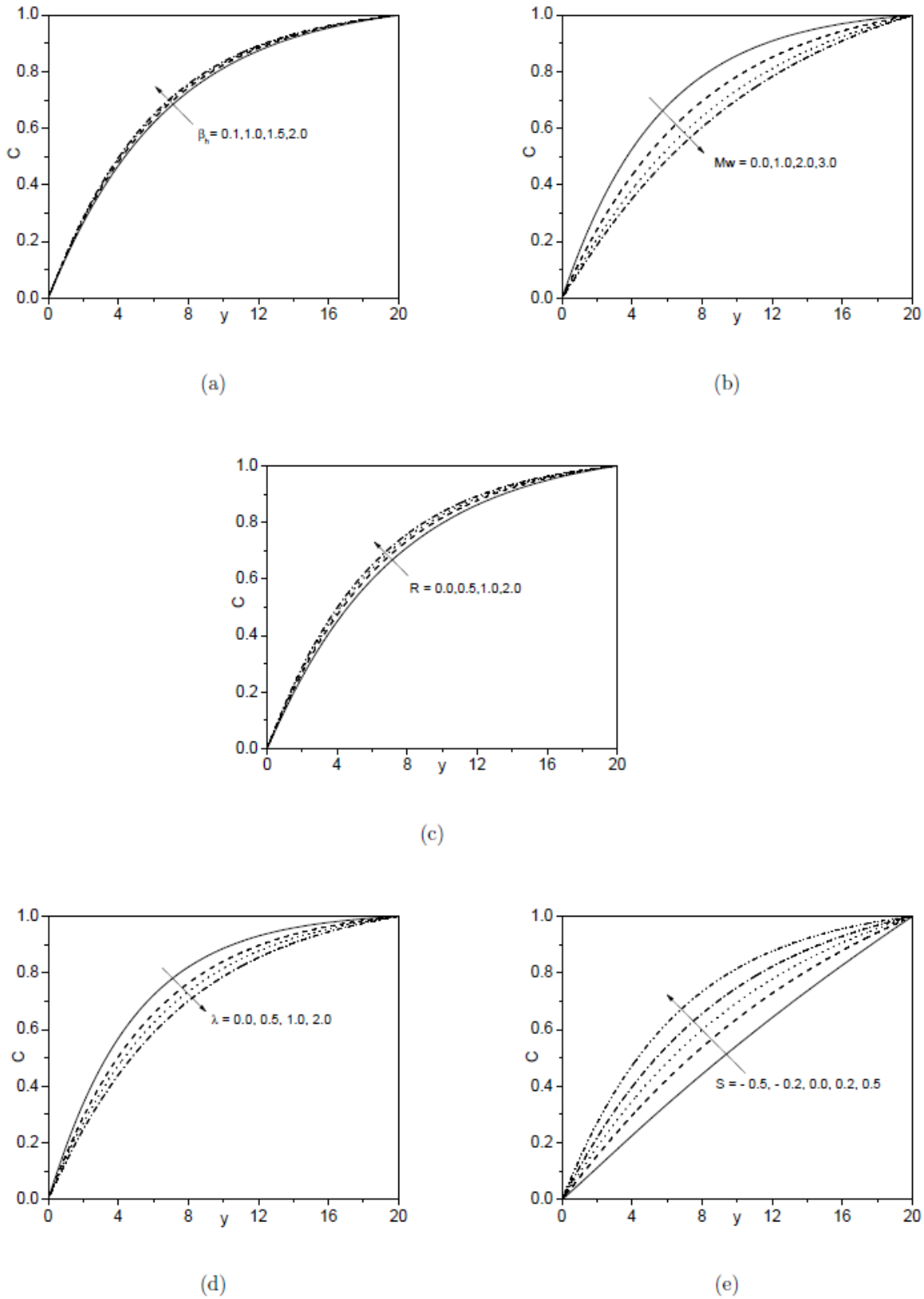

(a) (b)

(c)

(d) (e)

Figure 5: Influence of (a) β_h (b) Mw, (c) R, (d) λ and (e) S on C.

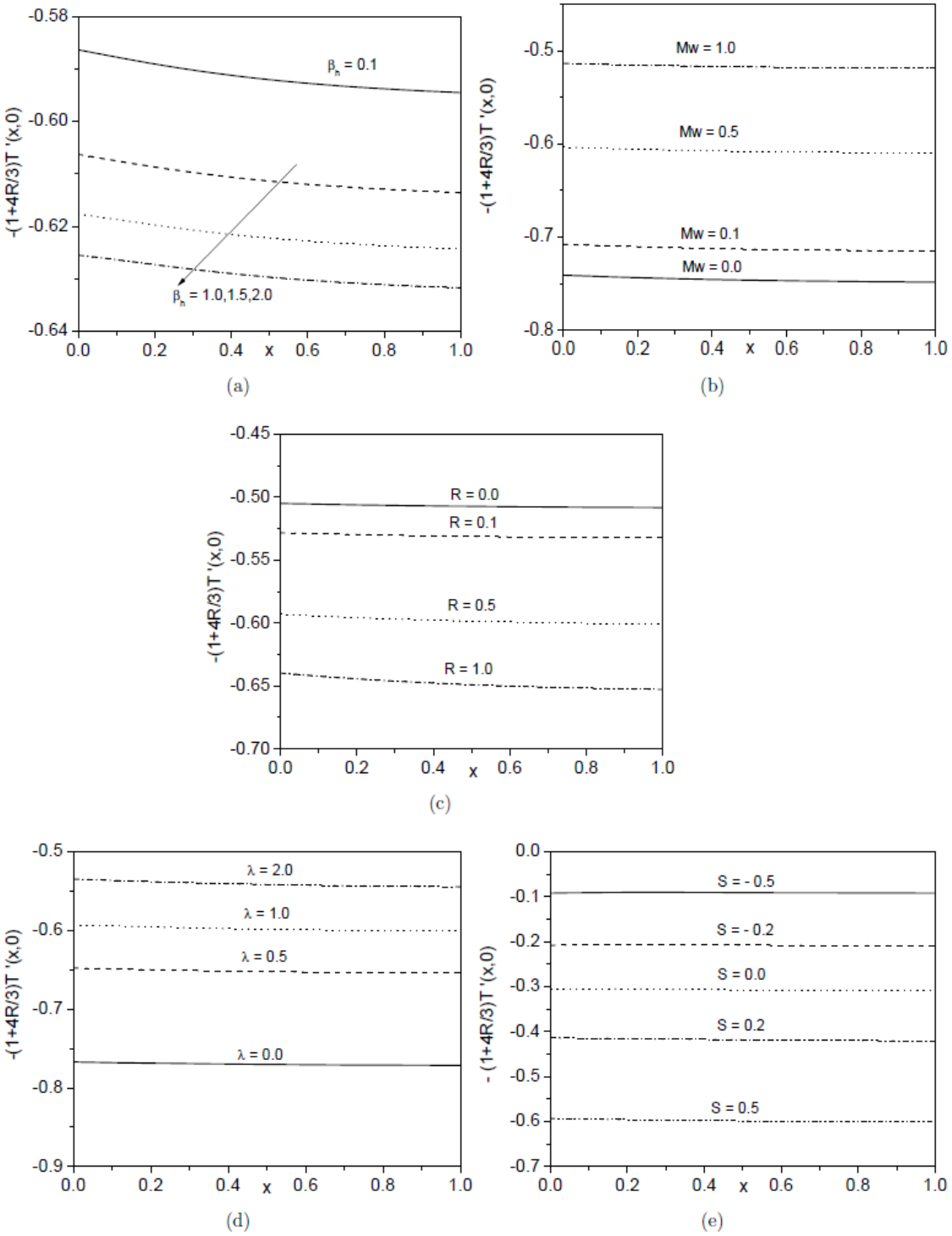

Figure 6: Influence of (a) β_h (b) Mw, (c) R, (d) λ and (e) S on $-(1+\frac{4R}{3})T'(x,0)$.

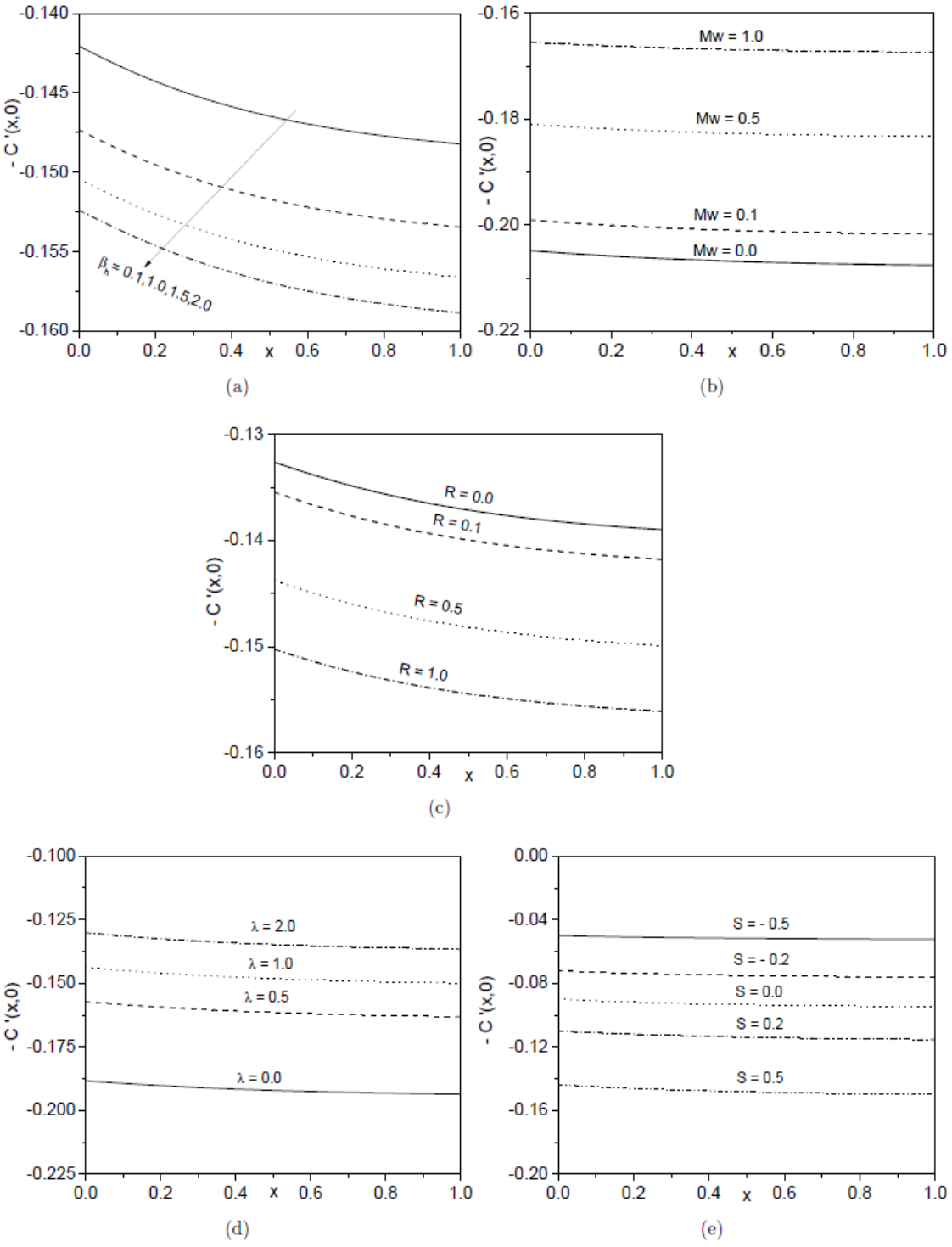

Figure 7: Influence of (a) β_h (b) Mw, (c) R, (d) λ and (e) S on $-C'(x,0)$.

Tabe 1: Effect of S, β_h, H_a, M_w, R and λ on $F''(x,0)$ and $W'(x,0)$.

S	β_h	H_a	M_w	R	λ	$F''(x,0)$	$W'(x,0)$
-0.2	1.0	0.5	1.0	0.5	0.5	-0.673300	0.084031
-0.1	1.0	0.5	1.0	0.5	0.5	-0.684868	0.084213
0.0	1.0	0.5	1.0	0.5	0.5	-0.696508	0.084261
0.1	1.0	0.5	1.0	0.5	0.5	-0.708232	0.084172
0.2	1.0	0.5	1.0	0.5	0.5	-0.720043	0.083949
0.5	0.0	0.5	1.0	0.5	0.5	-0.790537	0.000000
0.5	0.5	0.5	1.0	0.5	0.5	-0.777692	0.060241
0.5	1.0	0.5	1.0	0.5	0.5	-0.756019	0.082489
0.5	1.5	0.5	1.0	0.5	0.5	-0.740000	0.081943
0.5	1.0	0.0	1.0	0.5	0.5	-0.706334	0.000000
0.5	1.0	0.5	1.0	0.5	0.5	-0.756019	0.082489
0.5	1.0	1.0	1.0	0.5	0.5	-0.799511	0.138088
0.5	1.0	2.0	1.0	0.5	0.5	-0.871550	0.212770
0.5	1.0	0.5	0.0	0.5	0.5	-0.816379	0.077840
0.5	1.0	0.5	1.0	0.5	0.5	-0.756019	0.082489
0.5	1.0	0.5	2.0	0.5	0.5	-0.724416	0.083838
0.5	1.0	0.5	3.0	0.5	0.5	-0.704375	0.084226
0.5	1.0	0.5	1.0	0.0	0.5	-0.738263	0.083380
0.5	1.0	0.5	1.0	0.5	0.5	-0.756019	0.082489
0.5	1.0	0.5	1.0	1.0	0.5	-0.767282	0.081783
0.5	1.0	0.5	1.0	2.0	0.5	-0.780430	0.080825
0.5	1.0	0.5	1.0	0.5	0.0	-1.429483	0.112351
0.5	1.0	0.5	1.0	0.5	0.5	-0.756019	0.082489
0.5	1.0	0.5	1.0	0.5	1.0	-0.527896	0.068146
0.5	1.0	0.5	1.0	0.5	2.0	-0.335124	0.052413

- Both the velocities of the fluid reduces when the values of R, λ and S are increasing. While, increases with rise in the values of β_h and M_w.
- Temperature escalates with rise in β_h and S and falls with an increase in M_w, R and λ.
- As the Hall, radiation and suction parameter increases the concentration of the fluid increases and decreases with increase in the values of melting and velocity parameters.
- Both the skin-friction enhances with rise in M_w and β_h. Whereas reduces with a rise in fluid suction.
- The rate of heat absorption decreases as the values of melting and velocity slip parameter increases and increases with increase in Hall, radiation parameters and fluid suction.
- The rate of mass absorption escalates with a rise in the Hall, radiation parameters and fluid suction. But a reverse behavior is observed in presence of melting and velocity slip parameters.

REFERENCE

[1]. B.C. Sakiadis, "The boundary layer on a continuous flat surface", A.I.Ch.E. Journal., 7(2):221-225,1961.

[2]. E.M.Abo-Eldahad, M.A.El-Aziz, A.M.Salem, K.K.Jaber, "Hall current effect on MHD mixed convection flow from an inclined continuously stretching surface with blowing/suction and internal heat generation/absorption", Applied Mathematical Modelling., 31(9):1829-1846,2007.

[3]. S.Shateyi, S.S.Motsa, "Variable viscosity on magnetohydrodynamic fluid flow and heat transfer over an unsteady stretching surface with Hall effect", Boundary Value Problems., 2010(1),2010.

[4]. M.A.El-Aziz, "Flow and heat transfer over an unsteady stretching surface with Hall effect", Meccanica., 45(1):97-109,2010.

[5]. M.A.El-Aziz, T. Nabil, "Homotopy analysis solution of hydromagnetic mixed convection flow past an exponentially stretching sheet with Hall current", Mathematical Problems in Engineering., 2012:2012.

[6]. A.Zaib, S.Shafie, "Thermal diffusion and diffusion thermo effects on unsteady MHD free convection flow over a stretching surface considering Joule heating and viscous dissipation with thermal stratification, chemical reaction and Hall current", Journal of the Franklin Institute., 351(3):1268-1287,2014.

[7]. D.Srinivasacharya, P.Jagadeeshwar, "Flow over an exponentially stretching sheet with Hall, thermal radiation and chemical reaction effects", Frontiers in Heat and Mass Transfer., 9(37):1-10,2017.

[8]. D.Srinivasacharya, P.Jagadeeshwar, "Effect of variable viscosity, thermal conductivity and Hall currents on the flow over an exponentially stretching sheet with heat generation/absorption", International Journal of Energy for a Clean Environment., 19(1):1-17,2018.

[9]. E.M. Sparrow, R.D.Cess, "Radiation Heat Transfer, Series in Thermal and Fluids Engineering, Augmented ed. 1", McGraw-Hill.,1978. R. Angles and C. Gutierrez," Survey of graph database moDels",. ACM Comput. Surv., 40(1):1–39, 2008.

[10]. W.J.Minkowycz, E.M.Sparrow, "Local non-similar solution for natural convection on a vertical cylinder", Journal of Heat Transfer., 96:178-183,1974.

[11]. S.S.Motsa, S.Shateyi, "Successive Linearisation Solution of Free Convection Non-Darcy Flow with Heat and Mass Transfer", Advanced topics in mass transfer., 19:425-438,2011.

[12]. C.Canuto, M.Y.Hussaini, A.Quarteroni, T.A.Zang, "Spectral Methods: Fundamentals in Single Domains", Journal of Applied Mathematics and Mechanics.,87(1):2007.